Biosynthesis of metal nanoparticles using fungi and actinomycete

Murali Sastry[#,*], Absar Ahmad[§], M. Islam Khan[§] and Rajiv Kumar[†]

[#]Materials Chemistry Division, [§]Biochemical Sciences Division and [†]Catalysis Division, National Chemical Laboratory, Pashan Road, Pune 411 008, India

There is little doubt that nanomaterials will play a key role in many technologies of the future. One key aspect of nanotechnology concerns the development of reliable experimental protocols for the synthesis of nanomaterials over a range of chemical compositions, sizes and high monodispersity. In the context of the current drive to develop green technologies in materials synthesis, this aspect of nanotechnology assumes considerable importance. An attractive possibility is to use micro-organisms in the synthesis of nanoparticles. In this article, we provide a brief overview of the research efforts worldwide on the use of micro-organisms in the biosynthesis of inorganic nanoparticles, with particular emphasis on the recent and exciting results obtained at the National Chemical Laboratory, Pune on the biosynthesis of noble-metal nanoparticles using fungi and actinomycete. Some of the challenges in this emerging approach are highlighted.

THERE is tremendous current excitement in the study of nanoscale matter (matter having nanometre dimensions, 1 nm = 10^{-7} cm) with respect to their fundamental properties, organization to form superstructures and applications. The unusual physicochemical and optoelectronic properties of nanoparticles arise primarily due to confinement of electrons within particles of dimensions smaller than the bulk electron delocalization length, this process being termed quantum confinement[1–7]. The exotic properties of nanoparticles have been considered in applications such as optoelectronics[4,8], catalysis[9,10], reprography[11], single-electron transistors (SETs) and light emitters[12,13], nonlinear optical devices[14,15] and photoelectrochemical applications[16]. Magnetic nanoparticles are being viewed with interest from a fundamental point of view (superparamagnetism in the nanoparticles)[17] as well as in applications such as magnetic memory storage devices[18], magnetic resonance image enhancement[19] and magnetic refrigeration[20]. The ability to tune the optical absorption/emission properties of semiconductor nanoparticles (the so-called quantum dots) by simple variation in nanoparticle size is particularly attractive in the facile band-gap engineering of materials[21] and the growth of quantum dot lasers[22]. More recently, nanoscale matter has been looked at with interest for potential application in nanocomputers, synthesis of advanced materials, energy storage devices, electronic and optical displays, chemical and biosensors as well as biomedical devices[23]. Recognizing the importance of nanomaterials in key future technologies[24], many countries have launched major initiatives into the development of a strong fundamental and applied knowledge base in the area of nanotechnology[24]. It certainly does appear that 'there's plenty of room at the bottom'[25] in this fascinating area.

*For correspondence. (e-mail: sastry@ems.ncl.res.in)

Recent development of bio-based nanomaterials synthesis protocols

An important area of research in nanotechnology deals with the synthesis of nanoparticles of different chemical compositions, sizes and controlled monodispersity. Indeed, nanoparticle shape control is a recent addition to the list of demands being made of newly emerging synthesis methods. Currently, there is a growing need to develop environmentally benign nanoparticle synthesis processes that do not use toxic chemicals in the synthesis protocol. As a result, researchers in the field of nanoparticle synthesis and assembly have turned to biological systems for inspiration. This is not surprising given that many organisms, both unicellular and multicellular, are known to produce inorganic materials either intra- or extra-cellularly[26,27]. Some well-known examples of bio-organisms synthesizing inorganic materials include magnetotactic bacteria (which synthesize magnetite nanoparticles)[28–30], diatoms (which synthesize siliceous materials)[31–33] and S-layer bacteria (which produce gypsum and calcium carbonate layers)[34,35]. The secrets gleaned from nature have led to the development of biomimetic approaches for the growth of advanced nanomaterials.

Even though many biotechnological applications such as remediation of toxic metals employ micro-organisms such as bacteria[36] and yeast[37] (the detoxification often occurring via reduction of the metal ions/formation of metal sulphides), it is only relatively recently that materials scientists have been viewing with interest such micro-organisms as possible eco-friendly nanofactories[38,39]. Beveridge and co-workers[38–40] have demonstrated that gold particles of nanoscale dimensions may be readily precipitated within bacterial cells by incubation of the cells with Au^{3+} ions. Tanja Klaus and co-workers[41–43]

have shown that the bacteria *Pseudomonas stutzeri* AG259 isolated from a silver mine, when placed in a concentrated aqueous solution of $AgNO_3$, resulted in the reduction of the Ag^+ ions and formation of silver nanoparticles of well-defined size and distinct morphology within the periplasmic space of the bacteria. Taking this approach a step further, they have shown that biocomposites of nanocrystalline silver and the bacteria may be thermally treated to yield a carbonaceous (cermet) nanomaterial with interesting optical properties for potential application in functional thin-film coatings[43]. The exact reaction mechanism leading to the formation of silver nanoparticles by this species of silver-resistant bacteria is yet to be elucidated. In an interesting recent study, Nair and Pradeep[44] have demonstrated that bacteria not normally exposed to large concentrations of metal ions may also be used to grow nanoparticles. Nair and Pradeep have shown that *Lactobacillus* strains present in buttermilk, when challenged with silver and gold ions, resulted in the large-scale production of metal nanoparticles within the bacterial cells. They also showed that exposure of lactic acid bacteria present in the whey of buttermilk to mixtures of gold and silver ions could be used to grow nanoparticles of alloys of gold and silver[44]. Recently, Jose-Yacaman and co-workers[45,46] have shown that gold and silver nanoparticles may be synthesized in live alfalfa plants by gold and silver uptake from solid media. In addition to metal nanoparticles, there is much interest in the development of protocols for the synthesis of semiconductor nanoparticles such as CdS for application as quantum-dot fluorescent biomarkers in cell labelling[47]. Simple variation of the particle size enables tailoring of the band gap and consequently, the colour of the quantum dot during UV-light irradiation[47]. Bacteria and yeast have been used with success in the synthesis of CdS and PbS nanoparticles[48–52]. Holmes and co-workers[49] have shown that the bacterium, *Klebsiella aerogenes* when exposed to Cd^{2+} ions resulted in the intracellular formation of CdS nanoparticles in the size range 20–200 nm. They also showed that the composition of the nanoparticles formed was a strong function of buffered growth medium for the bacteria. Based on an extensive screening programme, Kowshik and co-workers[51] have identified the yeast, *Torulopsis* sp. as being capable of intracellular synthesis of nanoscale PbS crystallites when exposed to aqueous Pb^{2+} ions. The PbS nanoparticles were extracted from the biomass by freeze-thawing and analysed by a variety of techniques. In the final analysis, biogenic nanoparticles would have to compete with chemically synthesized nanoparticles in terms of performance for device applications. Recognizing this important issue, Kowshik *et al.*[52] have shown that CdS quantum dots synthesized intracellularly in *Schizosaccharomyces pombe* yeast cells exhibit ideal diode characteristics. Biogenic CdS nanoparticles in the size range 1–1.5 nm were used in the fabrication of a heterojunction with poly(*p*-phenylenevinylene). Such a diode exhibited 75 mA/cm^2 current in the forward bias mode at 10 V, while breakdown occurred at 15 V in the reverse direction. As can be seen from the above, the use of micro-organisms in the deliberate synthesis of nanoparticles is a relatively new and exciting area of research with considerable potential for development.

In a break from tradition, which has to a large extent relied on the use of prokaryotes such as bacteria in the synthesis of nanoparticles, we have recently embarked on a highly interdisciplinary programme at the National Chemical Laboratory (NCL), Pune aimed at investigating whether eukaryotic organisms such as fungi may be used to grow nanoparticles of different chemical compositions and sizes. A number of different genera of fungi have been investigated in this two-year effort (close to 200 different genera of fungi), and it has been shown that fungi are extremely good candidates in the synthesis of metal and metal sulphide nanoparticles. From this exhaustive study, we have observed that two different genera of fungi, *Verticillium* sp. and *Fusarium oxysporum*, when exposed to aqueous gold and silver ions, reduced the metal ions fairly rapidly. In the case of *Verticillium* sp., reduction of the metal ions occurred intracellularly leading to the formation of gold[53] and silver[54] nanoparticles in the size range 2–20 nm. To our pleasant surprise, *F. oxysporum* behaved considerably differently, the reduction of the metal ions occurring extracellularly resulting in the rapid formation of highly stable gold[55] and silver[56] nanoparticles of 2–50 nm dimensions. While we will not discuss the formation of metal sulphide nanoparticles by fungi in this article, the versatility of the approach is illustrated by the fact that extremely stable quantum dots of CdS may be formed extracellularly by challenging the fungus *F. oxysporum* with aqueous $CdSO_4$ solution[57]. The quantum dots are formed by reaction of Cd^{2+} ions with sulphide ions that are produced by the enzymatic reduction of sulphate ions to sulphide ions – the fungus thus plays the role of an enzyme source, in this case sulphate reductases[57]. In a bid to achieve better size and shape control, we have recently enlarged the scope of our studies to include organisms such as actinomycetes in the synthesis of metal nanoparticles[58]. In the remainder of this article, we illustrate the nanoparticle biosynthesis methods developed at NCL through two examples: intracellular growth of silver nanoparticles in *Verticillium* sp.[54] and use of the extremophilic actinomycete, *Thermomonospora* sp. in the extracellular growth of gold nanocrystals[58].

Biosynthesis of silver and gold nanoparticles using fungi and actinomycete

Intracellular synthesis of silver nanoparticles using Verticillium sp.

As briefly mentioned above, we have observed that the fungus *Verticillium* sp. when challenged with Ag^+ and

$AuCl_4^-$ ions leads to their reduction and accumulation as silver and gold nanoparticles within the fungal biomass. The acidophillic fungus, *Verticillium* sp., was isolated from the *Taxus* plant and maintained on potato-dextrose agar slants at 25°C. The fungus was grown in 500 ml Erlenmeyer flasks each containing 100 ml MGYP medium, composed of malt extract (0.3%), glucose (1.0%), yeast extract (0.3%), and peptone (0.5%) at 25–28°C under shaking condition (200 rpm) for 96 h. After 96 h of fermentation, mycelia were separated from the culture broth by centrifugation (5000 rpm) at 10°C for 20 min and the settled mycelia were washed thrice with sterile distilled water. Ten grams of the harvested mycelial mass was then re-suspended in 100 ml of 2×10^{-4} aqueous $AgNO_3$ solution in 500 ml Erlenmeyer flasks at pH 5.5–6.0. The whole mixture was thereafter put into a shaker at 28°C (200 rpm) and the reaction carried out for a period of 72 h. The bio-transformation was routinely monitored by visual inspection of the biomass as well as measurement of the UV-vis spectra from the fungal cells.

Thin sections of the *Verticillium* cells after reaction with Ag^+ ions in the manner described above were prepared for transmission electron microscopy (TEM) analysis as follows. Approximately 1 mm^3 bits of the Ag nano-*Verticillium* biomass were taken and fixed in 2.5% glutaraldehyde in distilled water for 2 h at room temperature. After fixation, the cells were sedimented (1500 rpm, 10 min) and washed thrice with distilled water. Without postfixation, the pellet was subjected to dehydration with 30, 50, 70 and 90% ethanol for 15 min at each concentration followed by two changes in absolute ethanol. Since ethanol does not possess good miscibility with epoxy resins, propylene oxide was used as a linking agent. The dehydrated pellet was kept in propylene oxide for 15 min following which the infiltration of the resin was done by placing the pellet in a 1 : 1 mixture of propylene oxide and Epon 812 overnight at room temperature. Embedding was carried out using a mixture of the resin (Epon 812) and hardeners (DDSA – dodecynyl succinic anhydride and MNA – methyl nadic anhydride) in the ratio 1 : 1.5. To this, two drops of tridimethylaminomethyl phenol (DMP30) was added to accelerate the polymerization process. Polymerization was carried out using this mixture at 60°C for three days. Ultrathin sections were cut using an ultramicrotome (Leica Ultracut UCT) and were taken on copper TEM grids (40 µm × 40 µm mesh size). The sections were slightly stained with uranyl acetate and lead citrate prior to TEM analysis. TEM measurements were carried out on a JEOL Model 1200EX instrument operated at an accelerating voltage of 60 kV. A low operating voltage was used to minimize damage to the thin sections by electron beam heating.

Verticillium fungal biomass before and after exposure to aqueous $AgNO_3$ solution for a period of 72 h is shown in Figure 1 *a* and *b*, respectively. The appearance of a dark brown colour in the fungal biomass after reaction with Ag^+ ions is a clear indicator of the reduction of the metal ions and formation of silver nanoparticles in the fungal biomass. Gold and silver nanoparticles exhibit striking colours (pink to blue for gold and light yellow to brown for silver) due to excitation of surface plasmon vibrations in the particles[59], and thus provide a convenient means of visually determining their presence in the fungal biomass. The growth of silver nanoparticles occurred only *within the fungal biomass* and not extracellularly, and is an interesting feature of this particular fungus. Figure 1 *c* shows the UV-vis spectra recorded from a film of the fungal cells before (curve 1) and after immersion in 10^{-4} M $AgNO_3$ solution for 72 h (curve 5). While there is no evidence of absorption in the spectral window 400–800 nm in the case of the as-harvested fungal cells, the fungal cells exposed to Ag^+ ions show a distinct and fairly broad absorption band centred at ca. 450 nm. The presence of the broad resonance indicates an aggregated structure of the silver particles in the film. A possible mechanism for the presence of silver nanoparticles in the fungal biomass could be the extracellular reduction of the Ag^+ ions in solution followed by precipitation onto the cells. UV-vis spectra recorded from the aqueous $AgNO_3$ solution after 6, 24 and 48 h of reaction with the biomass are shown as curves 2, 3 and 4, respectively in Figure 1 *c*. The curves have been displaced vertically for clarity. It is clear that there is negligible pres-

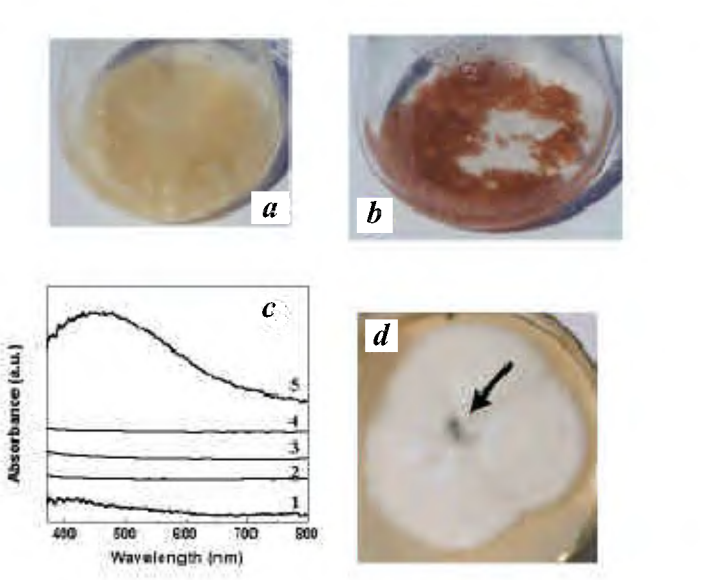

Figure 1. Conical flasks containing *Verticillium* biomass in aqueous solution of 1×10^{-4} M $AgNO_3$ at the beginning of the reaction (***a***) and after 72 h of reaction (***b***). ***c***, UV-vis spectra recorded from films of the fungal cells before (curve 1) and after immersion in 10^{-4} M aqueous $AgNO_3$ solution for 72 h (curve 5). Curves 2–4 correspond to spectra recorded from the $AgNO_3$ phase after 6, 24 and 48 h of exposure to the biomass respectively. ***d***, Growth of *Verticillium* after reaction with Ag^+ ions for 72 h. Dark core (indicated by arrow) is the seed Ag nano-*Verticillium* biofilm which grew to cover the surface of the agar plate (whitish mass) within one week. (Reprinted with permission from ref. 54, © 2001 American Chemical Society).

ence of silver particles in solution, thus distinctly pointing to intracellular/surface reduction of the Ag^+ ions as the most probable mechanism for the synthesis of silver nanoparticles by the fungus.

In the case of bacteria, most metal ions are toxic and therefore, reduction of the ions or formation of water insoluble complexes is a defence mechanism developed by bacteria to overcome such toxicity. In the case of fungi, which are normally not exposed to large concentrations of metal ions, the reduction of silver ions described above is surprising. It would be of interest to establish whether silver ions are toxic to *Verticillium* sp. Figure 1 *d* shows a small amount of the Ag nano-*Verticillium* biomass (dark core identified by an arrow) placed on an agar plate in the culture medium for one week. It is observed that the cells multiply and almost completely cover the agar plate of 8 cm diameter in one week (white mass). The *Verticillium* clearly does not die on either exposure to Ag^+ ions or after washing prior to measurement. Thus, the full capability of using micro-organisms in the synthesis of nanoscale materials may be realized if their ability to multiply (and cover large surface areas) is not compromised on exposure to metal ions as demonstrated in this work.

Figure 2 *a* shows a scanning electron microscopy (SEM) picture of *Verticillium* sp. cells after exposure to 10^{-4} M aqueous $AgNO_3$ solution for 72 h. (SEM measurements of the Ag nano-*Verticillium* sp. biomass were carried out on a Leica Stereoscan-440 scanning electron microscope equipped with a Phoenix EDAX attachment.) The highly filamentary nature of the mycelia is clearly seen in the figure. The presence of uniformly distributed silver nanoparticles on the surface of the fungal cells is observed, indicating that the nanoparticles formed by the reduction of Ag^+ ions are bound to the surface of the cells. The silver nanoparticles seen outside the mycelia may be due to weakly bound silver nanoparticles dislodged from the biomass during preparation of the films for SEM investigation, which it may be recalled, involves washing the biomass thrice with distilled water. Figure 2 *b* shows the EDAX (energy dispersive analysis of X-rays) spectrum recorded in the spot-profile mode from one of the densely populated silver nanoparticle regions on the surface of the fungal cells. Strong signals from the silver atoms in the nanoparticles are observed, while weaker signals from C, O, S, P, Mg and Na atoms were also recorded. The C, O, S, P, Mg and Na signals are likely to be due to X-ray emission from proteins/enzymes present in the cell wall of the biomass.

Information on the location of the silver nanoparticles relative to the fungal cells would be important in elucidating the mechanism of their formation and may be obtained by TEM analysis of thin sections of the Ag nano-*Verticillium* sp. cells. Figure 3 shows representative TEM images at various magnifications of the *Verticillium* cells. At lower magnification a number of mycelia can be observed, which on closer examination reveal assemblies of *Verticillium* cells within the mycelia (Figure 3 *a*). This image shows a number of dark spots on the cell walls as well as some spots within the cytoplasm. These dark spots correspond to silver nanoparticles synthesized by the fungus predominantly on the cell wall. Figure 3 *b* shows a slightly higher magnification image of the junction between two mycelia, wherein the individual cells are more clearly resolved. A number of silver particles can be seen on the mycelia wall surface. The mycelia in the upper right corner also shows an individual *Verticillium* cell with silver particles clearly bound to the surface of the cytoplasmic membrane (some of them identified by arrows in the figure). Analysis of the size of the silver nanoparticles from many different TEM images of the Ag nano-*Verticillium* cells yielded a particle diameter of 25 ± 12 nm. In this analysis of the silver particle size distribution, larger particles observed in the cell cytoplasm were excluded.

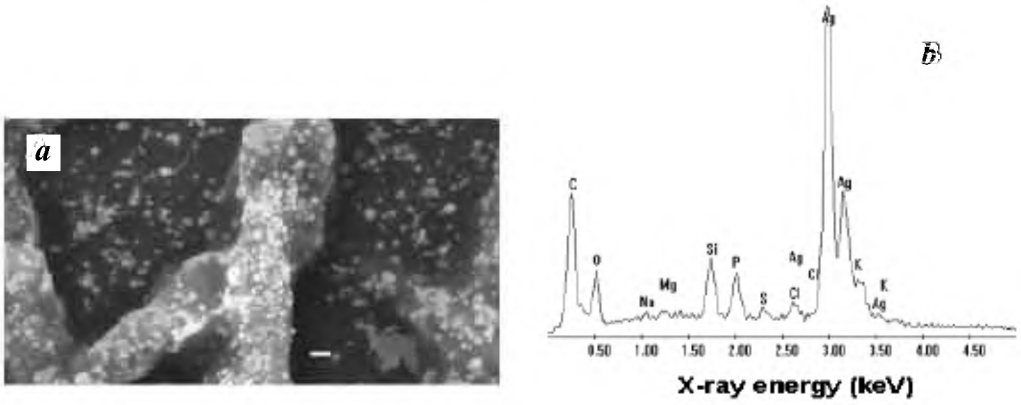

Figure 2. ***a***, SEM image of the *Verticillium* fungal cells after immersion in 10^{-4} M aqueous $AgNO_3$ solution for 72 h (scale bar = 1 μm). ***b***, EDAX spectrum recorded from a film of fungal cells after formation of silver nanoparticles. Different X-ray emission peaks are labelled. (Reprinted with permission from ref. 54, © 2001 American Chemical Society.)

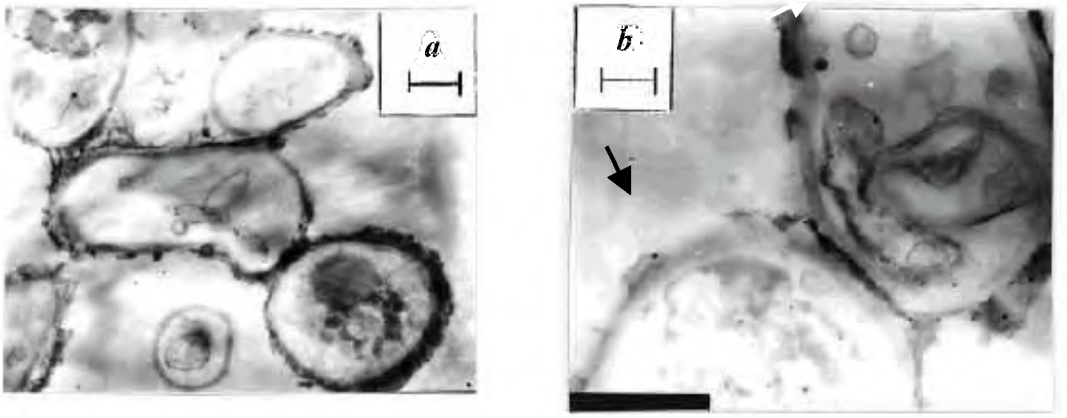

Figure 3 ***a***, ***b***. TEM images of thin sections of stained *Verticillium* sp. cells after reaction with Ag^+ ions for 72 h at different magnifications. Scale bars in (***a***) and (***b***) correspond to 1 μm and 500 nm, respectively. (Reprinted with permission from ref. 54, © 2001 American Chemical Society.)

The exact mechanism leading to the intracellular formation of gold[53] and silver[54] nanoparticles by challenging the fungus *Verticillium* sp. with the corresponding metal ions is not fully understood at the moment. We speculate that since the nanoparticles are formed on the surface of the mycelia and not in solution, the first step involves trapping of the Ag^+ ions on the surface of the fungal cells possibly via electrostatic interaction between the Ag^+ and negatively charged carboxylate groups in enzymes present in the cell wall of the mycelia. Thereafter, the silver ions are reduced by enzymes present in the cell wall leading to the formation of silver nuclei, which subsequently grow by further reduction of Ag^+ ions and accumulation on these nuclei. The TEM results indicate the presence of some silver nanoparticles on the cytoplasmic membrane as well as within the cytoplasm (Figure 3). It is possible that some Ag^+ ions diffuse through the cell wall and are reduced by enzymes present on the cytoplasmic membrane and within the cytoplasm. It may also be possible that some of the smaller silver nanoparticles diffuse across the cell wall to be trapped within the cytoplasm. Further work is currently in progress to clarify the mechanism and extend this process to the other metals such as Pt and alloys/bimetallics of Au–Pt, Ag–Au, etc.

Extracellular synthesis of gold nanoparticles by the actinomycete, Thermomonospora sp.

From the applications point of view, it would be important to harvest the metal nanoparticles formed within the fungal biomass. It is possible to release the intracellular silver and gold nanoparticles by ultrasound treatment of the Ag nano-*Verticillium* sp. biomass or by reaction with suitable detergents. However, it would be far more practical if the metal ions exposed to the fungus could be reduced *outside* the fungal biomass, leading to the formation of metal nanoparticle in solution. As mentioned briefly earlier, the fungus *F. oxysporum* when exposed to metal ions releases enzymes that reduce the metal ions to yield highly stable nanoparticles in solution[55,56]. The monodispersity of the silver/gold nanoparticles produced either intra- or extracellularly was not very high (~40–50%) and is thus far inferior to that obtained by conventional chemical methods (5–15%). More by chance than design, we observed that the extremophilic actinomycete, *Thermomonospora* sp. when exposed to gold ions reduced the metal ions extracellularly, yielding gold nanoparticles with a much improved polydispersity[58]. (Extremophiles are micro-organisms which thrive under conditions that are lethal to human beings such as extremes of temperature – from –14°C (psychrophiles), 45°C (thermophiles) to 110°C (hyperthermophiles); extremes of pH – from 1 (acidophiles) to 9 (alkalophiles); very high pressure (barophiles); non-aqueous environment containing 100% organic solvents; excess heavy metal concentration, etc. These micro-organisms have developed numerous special adaptations to survive in such extreme habitats, which include new mechanisms of energy transduction, regulating intracellular environment and metabolism, maintaining the structure and functioning of membrane and enzymes, etc. Actinomycetes are micro-organisms that share important characteristics of fungi and prokaryotes such as bacteria[60]. Even though they are classified as prokaryotes due to their close affinity with mycobacteria and the coryneforms (and thus amenable to genetic manipulation by modern recombinant DNA techniques), they were originally designated as 'ray fungi' (Strahlenpilze). Focus on actinomycetes has primarily centred on their phenomenal ability to produce secondary metabolites such as antibiotics[61].

A novel alkalothermophilic (extremophilic) actinomycete, *Thermomonospora* sp. having optimum growth at pH 9 and 50°C was isolated from self-heating compost in

the Barabanki district, Uttar Pradesh, India. This actinomycete was maintained on MGYP agar slants. Stock cultures were maintained by subculturing at monthly intervals. After growing the actinomycete at pH 9 and 50°C for four days, the slants were preserved at 15°C. From an actively growing stock culture, subcultures were made on fresh slants and after four days incubation at pH 9 and 50°C they were used as the starting material for fermentation experiments. For the synthesis of gold nanoparticles, the actinomycete was grown in 250 ml Erlenmeyer flasks containing 50 ml MGYP medium which is composed of malt extract (0.3%), glucose (1%), yeast extract (0.3%) and peptone (0.5%). Sterile 10% sodium carbonate was used to adjust the pH of the medium to 9. After adjusting the pH of the medium, the culture was grown with continuous shaking on a rotary shaker (200 rpm) at 50°C for 96 h. After 96 h of fermentation, mycelia (cells) were separated from the culture broth by centrifugation (5000 rpm) at 20°C for 20 min and then the mycelia was washed thrice with sterile distilled water under sterile conditions. The harvested mycelial mass (10 g of wet mycelia) was then resuspended in 50 ml of 10^{-3} M aqueous $AuCl_4$ solution in 250 ml Erlenmeyer flasks at pH 9. The whole mixture was put into a shaker at 50°C (200 rpm) and maintained in the dark. The bioreduction of the $AuCl_4^-$ ions in solution was monitored by periodic sampling of aliquots (2 ml) of the aqueous component and measuring the UV-vis spectra of the solution. Samples for TEM analysis were prepared on carbon-coated copper TEM grids. The films on the TEM grids were allowed to stand for 2 min following which the extra solution was removed using a blotting paper and the grid was allowed to dry prior to measurement. Fourier transform infrared (FTIR) spectroscopy measurements of drop-coated films of the chloroauric acid solution after 120 h of reaction with the biomass on Si (111) substrates were carried out on a Shimadzu 8201-PC instrument in the diffuse reflectance mode at a resolution of 4 cm^{-1}.

In order to identify the number of proteins secreted by the actinomycete and their molecular weights, the actinomycete biomass [10.0 g wet mycelia (cells)] was resuspended in 100 ml of sterile distilled water for a period of four days. The mycelia were then removed by centrifugation and the aqueous supernatant thus obtained was concentrated by ultrafiltration using a YM3 (molecular weight cut-off = 3K) membrane and then dialysed thoroughly against distilled water using a 3K cut-off dialysis bag. This concentrated aqueous extract containing protein was analysed by PAGE (polyacrylamide gel electrophoresis) carried out at pH 8.3, according to the procedure of Laemmli[62].

Figure 4 *a* shows the UV-vis spectra recorded from the aqueous chloroauric acid–actinomycete reaction medium as a function of time of reaction. It is observed that the gold surface plasmon band occurs at ca. 520 nm and steadily increases in intensity as a function of time of reaction. Complete reduction of the $AuCl_4^-$ ions occurs after nearly 120 h of reaction, indicating that it is an extremely slow process. Chloroauric acid solution after completion of the reaction is shown in Figure 4 *a* (inset). An intense red colour is observed, showing the formation of gold nanoparticles. As indicated in the experimental section, the bioreduction was carried out in the dark and clearly, the formation of gold nanoparticles is due to the actinomycete biomass. The fact that the surface plasmon band in the gold nanoparticle solution remains close to 520 nm throughout the reaction period indicates that the particles are dispersed in the aqueous solution, with no evidence for aggregation. After completion of the reaction, the gold nanoparticle solution was separated from the actinomycete biomass and tested for stability. It was observed that the nanoparticle solution was stable for more than six months, with little signs of aggregation (as determined by UV-vis spectroscopy measurements) even at the end of this period. The particles are thus stabilized in solution by a capping agent, likely to be proteins secreted by the biomass (see FTIR results below). The biomass was colourless, indicating that the reduction of the gold ions took place extracellularly.

Figure 4 *b* shows the FTIR spectrum recorded from the chloroauric acid solution after reaction with *Thermomonospora* sp. for 120 h. Two bands are seen at 1660 and 1530 cm^{-1}. These bands may be assigned to the amide I and II bands of proteins, respectively. It is well known that proteins can bind to gold nanoparticles either through free amine groups or cysteine residues in the proteins[63] and therefore, stabilization of the gold nanoparticles by surface-bound proteins is a possibility. The exact mechanism leading to the reduction of metal ions is yet to be elucidated for this micro-organism. As a first step in this direction, we have analysed the proteins released into water by the actinomycete in terms of the number of different proteins secreted and their molecular weights. Preliminary gel electrophoresis measurements indicate that the actinomycete secretes four distinct proteins of molecular masses between 80 and 10 kDa. We believe that one or more of these proteins may be enzymes that reduce chloroaurate ions and cap the gold nanoparticles formed by the reduction process. It is also possible that the capping and stabilization of the gold nanoparticles is effected by a different protein. We are currently separating and concentrating the different proteins released by the actinomycete, *Thermomonospora* sp. to test and identify the ones active in the above processes.

Figure 5 *a* and *b* shows TEM pictures recorded from drop-coated films of gold nanoparticles synthesized using *Thermomonospora* sp. after reacting chloroauric acid with the biomass for 120 h. The low-magnification TEM image clearly shows dense assembly of uniformly-sized gold nanoparticles (Figure 5 *a*). Indeed, the whole surface of the grid was evenly covered with gold nanoparticles as

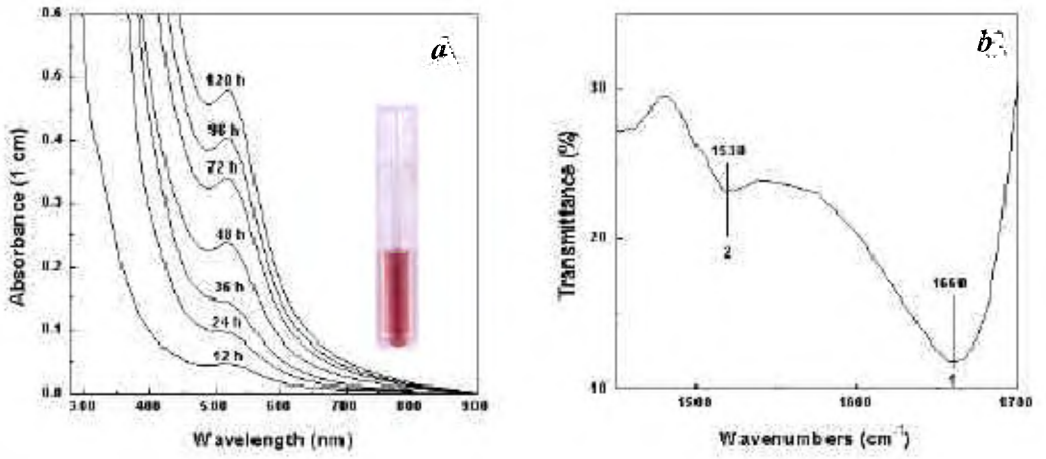

Figure 4. ***a***, UV-vis spectra recorded as a function of time of reaction of 10^{-4} M aqueous solution of $HAuCl_4$ with *Thermomonospora* sp. biomass. (Inset) Test tube of nanoparticle solution formed at the end of the reaction (120 h). ***b***, FTIR spectrum recorded from drop-cast films of the chloroauric acid solution after reaction with *Thermomonospora* sp. biomass for 120 h. The amide I and II bands are identified. (Reprinted with permission from ref. 58, © 2001 American Chemical Society).

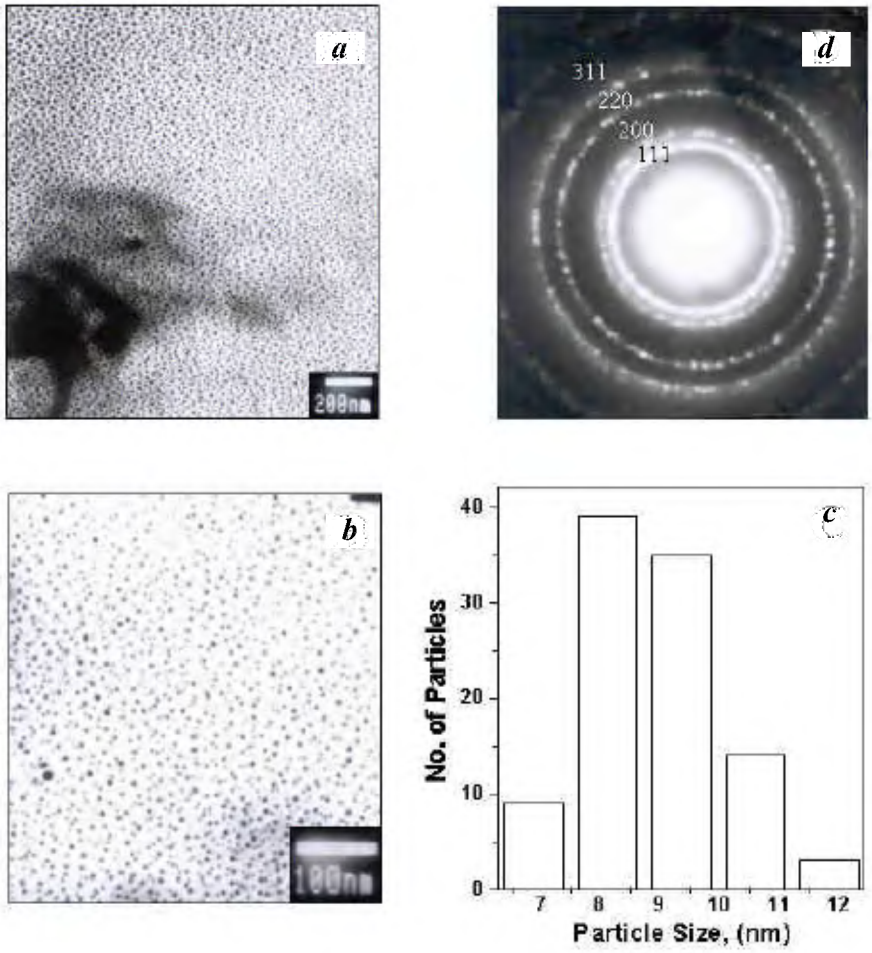

Figure 5. ***a*** and ***b***, TEM micrographs recorded from drop-cast films of gold nanoparticle solution formed by the reaction of chloroauric acid solution with *Thermomonospora* sp. biomass for 120 h at different magnifications. ***c***, Particle size distribution histogram determined from the TEM micrograph shown in Figure 2 *b*. ***d***, Selected area diffraction pattern recorded from the gold nanoparticles shown in Figure 2 *b*. (Reprinted with permission from ref. 58, © 2001 American Chemical Society).

shown in this image. At slightly higher magnification, a better idea of the morphology and size of the particles may be had (Figure 5 *b*). The particles are essentially spherical and appear to be reasonably monodisperse. The particle size histogram derived from the particles shown in this image and other similar images is given in Figure 5 *c*. It can be seen that the average particle size is ca. 8 nm, with some particles of 9–10 nm size and a very small percentage having diameters 7–12 nm. Thus, a significant improvement in the monodispersity has been achieved using actinomycete. Whether the size and dispersity control is a consequence of larger amounts of proteins/enzymes secreted by *Thermomonospora* sp. in comparison with *F. oxysporum* remains to be established. Another distinct possibility is that the nature and strength of interaction of different proteins with different crystallographic faces of gold nanocrystals may vary – this may lead to complex morphologies and size control. It is also to be noted that the synthesis conditions are different in both cases. In the case of actinomycete, the reaction is carried out under alkaline conditions and at slightly elevated temperatures. Under these extreme conditions, fungi such as *F. oxysporum* would not survive. The use of extreme biological conditions in the synthesis could also be a contributory factor in the size and monodispersity control observed using actinomycetes. Figure 5 *d* shows the selected area electron diffraction pattern obtained from the gold nanoparticles shown Figure 5 *b*. The Scherrer ring pattern characteristic of face centred cubic gold is clearly observed, showing that the structures seen in the TEM images are nanocrystalline in nature.

Conclusions and future directions

In summary, a brief overview of the use of micro-organisms such as bacteria, yeasts, algae, fungi and actinomycetes in the biosynthesis of metal nanoparticles has been described, with particular emphasis on the work from NCL. We hope a case has been made for the serious study of micro-organisms in the synthesis of nanomaterials as a possible viable alternative to the more popular physical and chemical methods currently in vogue. The use of fungi and actinomycetes as sources of enzymes that can catalyse specific reactions leading to inorganic nanoparticles is a new and rational biosynthesis strategy that is being developed at NCL. Extracellular secretion of enzymes offers the advantage of obtaining large quantities in a relatively pure state, free from other cellular proteins associated with the organism and can be easily processed by filtering of the cells and isolating the enzyme for nanoparticles synthesis from cell-free filtrate. The use of specific enzymes secreted by organisms such as fungi in the synthesis of nanoparticles is exciting for the following reasons. The process can be extended to the synthesis of nanoparticles of different chemical compositions and indeed, different shapes and sizes by suitable identification of enzymes secreted by the fungi. Understanding the surface chemistry of the biogenic nanoparticles (i.e. nature of capping surfactants/peptides/proteins) would be equally important. This would then lead to the possibility of genetically engineering microbes to overexpress specific reducing molecules and capping agents and thereby, control the size and shape of the biogenic nanoparticles. The rational use of constrained environments within cells such as the periplasmic space and cytoplasmic vesicular compartments (e.g. magnetosomes) to modulate nanoparticle size and shape is an exciting possibility yet to be seriously explored. The fungal and actinomycete-mediated green chemistry approach towards the synthesis of nanoparticles has many advantages such as ease with which the process can be scaled up, economic viability, possibility of easily covering large surface areas by suitable growth of the mycelia, etc. The shift from bacteria to fungi as a means of developing natural 'nano-factories' has the added advantage that downstream processing and handling of the biomass would be much simpler. Compared to bacterial fermentations, in which the process technology involves the use of sophisticated equipment for getting clear filtrates from the colloidal broths, fungal broths can be easily filtered by filter press of similar simple equipment, thus saving considerable investment costs for equipment. Fungi have been found to be extremely efficient secretors of soluble protein and under optimized conditions of fermentations, mutant strains secrete up to 30 g per litre of extracellular protein. In the strains selected for enzyme fermentations, the desired enzyme constitutes the only component or at least forms the major ingredient of the secreted protein with high specific activities. It is this trait of high-level protein secretion, besides their eukaryotic nature, that has made fungi as favourite hosts for heterologous expression of high-value mammalian protein for manufacturing by fermentation. Further, compared to bacteria; fungi and actinomycetes are known to secrete much higher amounts of proteins, thereby significantly increasing the productivity of this biosynthetic approach.

Equally intriguing are questions related to the metal ion reduction/reaction process in cellular metabolism and whether the nanoparticles formed as by-products of the reduction process have any role to play in a cellular activity (such as magnetite in magnetotactic bacteria). Micro-organisms such as fungi are not normally exposed to high concentrations of metal ions such as Cd^{2+}, $AuCl_4^-$ and Ag^+. That they secrete enzymes when challenged, which are capable of metal-ion reduction and indeed conversion of sulphates to sulphides, suggests evolutionary processes are at play.

1. Fendler, J. H., *Membrane Mimetic Chemistry Approach to Advanced Materials*, Springer-Verlag, Berlin, 1992.
2. Henglein, A. and Bunseng, Ber., *Phys. Chem.*, 1995, **99**, 903–913.

3. Weller, H., *Angew. Chem., Int. Ed. Engl.*, 1993, **32**, 41–53.
4. Colvin, V. L., Schlamp, M. C. and Alivisatos, A. P., *Nature*, 1994, **370**, 354–357.
5. Brus, L. E., *J. Chem. Phys.*, 1984, **80**, 4403–4409.
6. Henglein, A., *J. Phys. Chem.*, 1993, **97**, 5457–5464.
7. Alivisatos, A. P., *Science*, 1996, **271**, 933–937.
8. Wang, Y. and Herron, N., *J. Phys. Chem.*, 1991, **95**, 525–532.
9. Schmid, G., *Chem. Rev.*, 1992, **92**, 1709–1727.
10. Hoffman, A. J., Mills, G., Yee, H. and Hoffman, M. R., *J. Phys. Chem.*, 1992, **96**, 5546–5552.
11. Hamilton, J. F. and Baetzold, R. C., *Science*, 1979, **205**, 1213–1220.
12. Klein, D. L., Roth, R., Lim, A. K. L., Alivisatos, A. P. and McEuen, P. L., *Nature*, 1997, **389**, 699–701.
13. Weller, H., *Angew. Chem., Int. Ed. Engl.*, 1998, **37**, 1658–1659.
14. Wang, Y., *Acc. Chem. Res.*, 1991, **24**, 133–139.
15. Yoffe, A. D., *Adv. Phys.*, 1993, **42**, 173–266.
16. Mansur, H. S., Grieser, F., Marychurch, M. S., Biggs, S., Urquhart, R. S. and Furlong, D. N., *J. Chem. Soc., Faraday Trans.*, 1995, **91**, 665–672.
17. Shi, J., Gider, S., Babcock, K. and Awschalom, D. D., *Science*, 1996, **271**, 937–941.
18. Symonds, J. L., *Phys. Today*, 1995, **48**, 26–32.
19. Bulte, J. W. M. *et al.*, *Invest. Radiol.*, 1994, **29**, 5214–5216.
20. Shull, R. D., McMichael, R. D. and Ritter, J. J., *Nanostruct. Mat.*, 1993, **2**, 205–211.
21. Fendler, J. H. and Meldrum, F., *Adv. Mater.*, 1995, **7**, 607–632.
22. Ledentsov, N. N. *et al.*, *J. Solid State Electron.*, 1996, **40**, 785–798.
23. *Chem. Eng. News*, 28 February 2002, and articles by Dagani, R. therein for coverage of the new applications envisaged for nanomaterials.
24. The interested reader is directed to the review of the current status of nanotechnology, applications and initiatives in various countries, which may be obtained at www.nano.gov.
25. The classic talk by Richard Feynman entitled 'There's plenty of room at the bottom' delivered at the annual meeting of the American Physical Society at the California Institute of Technology in 1959 is possibly the first serious exposition on the problem of manipulating nanoscale objects (the talk is available on the web at http://www.zyvex.com/nanotech/feynman.html).
26. Simkiss, K. and Wilbur, K. M., *Biomineralization*, Academic Press, New York, 1989.
27. Mann, S. (ed.), *Biomimetic Materials Chemistry*, VCH Publishers, 1996.
28. Lovley, D. R., Stolz, J. F., Nord, G. L. and Phillips, E. J. P., *Nature*, 1987, **330**, 252–254.
29. Spring, H. and Schleifer, K. H., *Sys.. Appl. Microbiol.*, 1995, **18**, 147–153.
30. Dickson, D. P. E., *J. Magn. Magn. Mater.*, 1999, **203**, 46–49.
31. Mann, S., *Nature*, 1993, **365**, 499–505.
32. Oliver, S., Kupermann, A., Coombs, N., Lough, A. and Ozin, G. A., *Nature*, 1995, **378**, 47–51.
33. Kroger, N., Deutzmann, R. and Sumper, M., *Science*, 1999, **286**, 1129–1132.
34. Pum, D. and Sleytr, U. B., *Trends Biotechnol.*, 1999, **17**, 8–12.
35. Sleytr, U. B., Messner, P., Pum, D. and Sara, M., *Angew. Chem., Int. Ed. Engl.*, 1999, **38**, 1034–1036.
36. Stephen, J. R. and Maenaughton, S. J., *Curr. Opin. Biotechnol.*, 1999, **10**, 230–233.
37. Mehra, R. K. and Winge, D. R., *J. Cell. Biochem.*, 1991, **45**, 30–40.
38. Southam, G. and Beveridge, T. J., *Geochim. Cosmochim. Acta*, 1996, **60**, 4369–4376.
39. Beveridge, T. J. and Murray, R. G. E., *J. Bacteriol.*, 1980, **141**, 876–887.
40. Fortin, D. and Beveridge, T. J., in *Biomineralization. From Biology to Biotechnology and Medical Applications* (ed. Baeuerien, E.), Wiley-VCH, Weinheim, 2000, p. 7.
41. Klaus, T., Joerger, R., Olsson, E. and Granqvist, C. G., *Proc. Natl. Acad. Sci. USA*, 1999, **96**, 13611–13614.
42. Klaus-Joerger, T., Joerger, R., Olsson, E. and Granqvist, C. G., *Trends Biotechnol.*, 2001, **19**, 15–20.
43. Joerger, R., Klaus, T. and Granqvist, C. G., *Adv. Mater.*, 2000, **12**, 407–409.
44. Nair, B. and Pradeep, T., *Cryst. Growth Des.*, 2002, **2**, 293–298.
45. Gardea-Torresdey, J. L., Parsons, J. G., Gomez, E., Peralta-Videa, J., Troiani, H. E., Santiago, P. and Yacaman, M. J., *Nano Lett.*, 2001, **2**, 397–401.
46. Gardea-Torresdey, J. L., Gomez, E., Peralta-Videa, J. R., Parsons, J. G., Troiani, H. and Jose-Yacaman, M., *Langmuir*, 2003, **19**, 1357–1361.
47. Chan, W. C. W., Maxwell, D. J., Gao, X., Bailey, R. E., Han, M. and Nie, S., *Curr. Opin. Biotechnol.*, 2002, **13**, 40–46.
48. Cunningham, D. P. and Lundie, L. L., *Appl. Environ. Microbiol.*, 1993, **59**, 7–14.
49. Holmes, J. D., Smith, P. R., Evans-Gowing, R., Richardson, D. J., Russell, D. A. and Sodeau, J. R., *Arch. Microbiol.*, 1995, **163**, 143–147.
50. Smith, P. R., Holmes, J. D., Richardson, D. J., Russell, D. A. and Sodeau, J. R., *J. Chem. Soc., Faraday Trans.*, 1998, **94**, 1235–1241.
51. Kowshik, M., Vogel, W., Urban, J., Kulkarni, S. K. and Paknikar, K. M., *Adv. Mater.*, 2002, **14**, 815–818.
52. Kowshik, M., Deshmukh, N., Vogel, W., Urban, J., Kulkarni, S. K. and Paknikar, K. M., *Biotechnol. Bioeng.*, 2002, **78**, 583–588.
53. Mukherjee, P. *et al.*, *Angew. Chem., Int. Ed. Engl.*, 2001, **40**, 3585–3588.
54. Mukherjee, P. *et al.*, *Nano Lett.*, 2001, **1**, 515–519.
55. Mukherjee, P., Senapati, S., Mandal, D., Ahmad, A., Khan, M. I., Kumar, R. and Sastry, M., *Chem. Biochem.*, 2002, **3**, 461–463.
56. Ahmad, A., Mukherjee, P., Senapati, S., Mandal, D., Khan, M. I., Kumar, R. and Sastry, M., *Colloid Surf. B*, 2003, **28**, 313–318.
57. Ahmad, A., Mukherjee, P., Mandal, D., Senapati, S., Khan, M. I., Kumar, R. and Sastry, M., *J. Am. Chem. Soc.*, 2002, **124**, 12108–12109.
58. Ahmad, A., Senapati, S., Khan, M. I., Kumar, R. and Sastry, M., *Langmuir*, 2003, **19**, 3550–3553.
59. Henglein, A., *J. Phys. Chem.*, 1993, **97**, 5457–5471.
60. Okami, Y., Beppu, T. and Ogawara, H. (eds), *Biology of Actinomycetes*, Japan Scientific Societies Press, Tokyo, 1988, vol. 88, p. 508.
61. Sasaki, T., Yoshida, J., Itoh, M., Gomi, S., Shomura, T. and Sezaki, M., *J. Antibiot.*, 1988, **41**, 835–842.
62. Laemmli, U. K., *Nature*, 1970, **227**, 680–685.
63. Gole, A., Dash, C., Ramachandran, V., Mandale, A. B., Sainkar, S. R., Rao, M. and Sastry, M., *Langmuir*, 2001, **17**, 1674–1679.

ACKNOWLEDGEMENTS. We thank Dr Priyabrata Mukherjee, S. Senapati and D. Mandal for their enthusiastic contributions to much of the experimental work. The SEM and TEM analyses of the nanofungi biocomposites were carried out by Dr S. R. Sainkar and Ms Renu Pasricha.

Received 27 February 2003; revised accepted 28 April 2003